Road Materials and Pavement Design, 2015
http://dx.doi.org/10.1080/14680629.2015.1028970

Taylor & Francis
Taylor & Francis Group

Laboratory investigation of the strength, stiffness, and thermal conductivity of fly ash and lime kiln dust stabilised clay subgrade materials

Xin Kang[a], Louis Ge[b*], Gi-Chun Kang[c] and Christopher Mathews[d]

[a]*Department of Civil, Architectural, and Environmental Engineering, Missouri University of Science and Technology, Rolla, MO, USA;* [b]*Department of Civil Engineering, National Taiwan University, Taipei, Taiwan;* [c]*Dam & Watershed Maintenance Department, K-water, Daedeok-Gu, Daejeon 306–711, Republic of Korea;* [d]*SCI Engineering, O'Fallon, IL, USA*

(*Received 8 October 2014; accepted 8 March 2015*)

The effectiveness of Class-C fly ash (FA) (ASTM C-618) and lime kiln dust (LKD) used in clay pavement base materials stabilisation has been investigated in this research. Proctor compaction test, unconfined compression test, and non-destructive test (Briaud compaction device (BCD) modulus and thermal conductivity) were carried out on the chemically modified soil. Test specimens were reconstituted by static compaction, constructed at optimum water content, and tested at various curing periods. Test results revealed that the addition of Class-C FA up to 20 wt% could effectively increase the dry unit weight from 16.8 to 17.4 kN/m^3 (105.0 to 108.3 pcf), improve the unconfined compressive strength (UCS, which increased from 181.2 to 497.2 kPa at the end of 28 days of curing), and raise the BCD modulus up to 40 MPa. The LKD was also found to be a good stabiliser for weak soil, which could raise the UCS and stiffness under relatively small mixing rations (4 and 8 wt%), but the dry unit weight decreased as the LKD mixing ratio increased. The thermal conductivity, however, decreased as the curing time and stabiliser mixing ratio increased. Parallel and series models were employed to understand the upper-and-lower bound of the mixtures' thermal conductivity. A thermal strength coupled empirical model which is based on the non-destructive testing results was developed to predict the UCS gain over curing time. The thermal conductivity and BCD modulus were also incorporated into a novel compaction quality check model. Based on the observed test data and regression analysis, both models were found to yield good results, indicating that they are robust tools for predicting the UCS and dry unit weight of chemically treated pavement base materials.

Keywords: fly ash; lime kiln dust; BCD modulus; proctor compaction; unconfined compressive strength; thermal conductivity

Introduction

Low strength and high compressibility clays are commonly encountered in pavement construction in Missouri State, USA. Instead of replacing the *in situ* soil by other earth materials, chemical stabilisers, such as Class-C fly ash (FA) and lime kiln dust (LKD), were found to have great beneficial potential in soil stabilisation due to their excellent self-cementing characteristics (e.g. Misra, 1998; Tuncer, Hector, & Craig, 2006). The FA-treated soil is typically strong and stiff, and the plasticity and shrink–swell potential could be reduced as well (e.g. Cokca, 2001; Puppala, Ramakrishna, & Hoyos, 2003; Tuncer et al., 2006). The stabilisation mechanism of Class-C

*Corresponding author. Email: louisge@ntu.edu.tw

FA was studied by several researchers, including Saylak, Mishra, Mejeoumov, and Shon (2008), Lloyd, Provis, and van Deventer (2009), Horpibulsuk, Rachan, and Raksachon (2009), and Shon, Saylak, and Mishra (2010). The hardening process of the mixture was primarily divided into two parts, the short-term effect and the long-term effect, respectively. The short-term effect takes place immediately as the FA is blended with soil. The long-term strength gain is attributed to the hydration of cementation material and the pozzolanic reaction because high quantities of lime (CaO), silica dioxide (SiO_2), and alumina trioxide (Al_2O_3) are contained in the FA. The strength and stiffness improvement are largely dependent on the long-term effect (Chitambira, 2004; Kamruzzaman, Chew, & Lee, 2009; Tan, Goh, & Yong, 2002). The studies of the strength gain and small stain stiffness improvement of chemically stabilised soil have been well documented in the literature; however, not many studies were found on investigating the thermal properties and small-strain modulus of the stabilised soils. The study of soil thermal properties has a significant relation to engineering applications (Abuel-Naga, Bergado, & Bouazza, 2008; Abu-Hamdeh & Reeder, 2000; Bachmann, Horton, Ren, & van der Ploeg, 2001; Balland & Arp, 2005; Brandon & Mitchell, 1989; Brandon, Mitchell, & Cameron, 1989). A literature review revealed that very limited studies were found to adopt the non-destructive testing method to monitor and control the filed compaction quality in engineering practice (Weidinger & Ge, 2009). Compared with destructive laboratory testing methods, such as unconfined compression shear, triaxial shear, and resilient modulus test, non-destructive testing (e.g. Briaud compaction device (BCD) modulus and thermal conductivity) showed its great features. The non-destructive testing is low in cost, simple and easy to carry out in the field, and reliable. The non-destructive testing method, thus, could be served as a convenient tool for continuously monitoring the strength and small-strain stiffness improvement of chemically treated geomaterials.

In summary, the objectives of the research are as follows: (1) Evaluate the effectiveness of self-cementing Class-C FA and LKD for clay pavement materials stabilisation by carrying out both destructive testing (unconfined compression strength) and non-destructive testing (which included BCD modulus and thermal conductivity); (2) investigate the physicochemical effects of FA and LKD on the hardening process of the stabilised soils; (3) correlate and compare the destructive testing results with non-destructive testing results on FA and LKD stabilised clay subgrade soils; and (4) develop mechanical and thermal coupled models to evaluate the unconfined compressive strength (UCS) gain and check the field compaction quality based on the non-destructive testing methods.

Test materials

Two different types of chemical stabilisers, the Class-C FA and LKD, were used in this study. Large quantities of FAs were generated by electrical power plants worldwide. Every year, only about 20–30% of generated FA is used as additives in cement and concrete as replacement materials. The rest of them are disposed in landfills and surface impoundments nationwide. Therefore, increasing the recycling percentage of FA is of great significance to the sustainable development and global energy market. In this research, different FA samples were first obtained from five thermo power plants in Missouri State. Set time tests (Kang, Kang, & Ge, 2013) were carried out to determine the proper setting time of the FA and served as a screening criterion for selecting the best FA stabiliser. The FA selected in this study was from LaBadie Power Plant in Washington, Missouri, USA. The chemical compositions and the engineering properties of the LaBadie FA are listed in Table 1.

LKD is a by-product from the Portland cement manufacturing process. It is estimated that about 2.5 million metric tons of high-calcium LKD is produced annually in the USA (Miller

Table 1. Percentage of chemical compositions in FA.

Chemicals	%
SiO_2	33.72
Al_2O_3	21.90
Fe_2O_3	7.15
CaO	25.31
MgO	4.48
SO_3	2.25
K_2O	0.41
P_2O_5	1.20
TiO_2	1.30
Na_2O	1.40
LOI	0.37

& Callaghan, 2004). The LKD is potentially useful in stabilising a variety of soils (i.e. sandy and clayey soils), which in turn is found to be a cost-effective way of recycling the by-product LKD. The addition of LKD in soil was found to increase the California bearing ratio value, improve the summary resilient modulus, and lower plastic strains (Cetin, Aydilek, & Guney, 2010). It was reported that LKD could be used together with quicklime for effective municipal sludge pasteurisation and stabilisation (Burnham, Hatfield, Bennett, & Logan, 1992; Heckel & Wahab, 1996). The LKD has also been successfully used in the stabilisation of subgrade soils, improvement of resilient modulus, and enhancement of the UCS (Daita, Drnevich, Kim, & Chen, 2006; Kang, Kang, Chang, & Louis, 2014; Solanki, Zaman, & Dean, 2010). The LKD used in this study was shipped from Mississippi Lime Company at St. Louis, Missouri, USA, which contains the key ingredients of lime (20–40% calcium oxide) and FA (8–15%) from the coal used to burn or calcinate the limestone to lime.

The clayey subgrade soil was obtained from a roadbase construction site in Atchison County, Missouri, USA. The plastic and liquid limits are 21 and 38, respectively. According to the unified soil classification system, the Atchison soil was classified as low plasticity clay (CL). The grain-size distribution curves of the soil, FA, and LKD are shown in Figure 1. The FA is gap graded

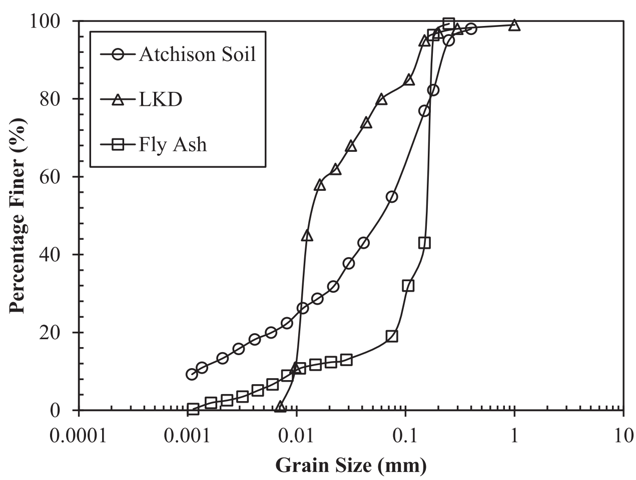

Figure 1. Grain-size distribution curves of clays and chemical additives.

Table 2. Summary of FA and LKD mixing ratios.

	Percentage by weight of soils and additives		
	Soils	Additives	
Test case	Atchison	FA	LKD
ACL0	100	–	–
AC10	90	10	–
AC15	85	15	–
AC20	80	20	–
AL04	96	–	4
AL08	92	–	8

and its grain-size distribution curve was located to the right, indicating that the FA was coarser. Table 2 gives the mixing ratios between the soil and the additives (The FA was taken as the *major chemical stabiliser* in this research; therefore, three mixing ratios were used. On the contrary, two mixing ratios of LKD were adopted in this research to identify the effectiveness of the LKD treatment). Typically, the FA mixing ratio was kept lower than 30% and the LKD mixing ratio was kept lower than 15% to prevent the development of desiccation cracks during sample curing.

Specimen preparation

The soil (sampled from Atchison County, Missouri, USA) was first air-dried and mechanically pulverised before passing through a #40 sieve (425 mm). The processed dry soil was mixed with FA and LKD by targeting mixture ratios and optimum water contents, and then well mixed. The FA/LKD soil mixtures were compacted into a 152.4-mm (6 in.) split proctor mould. After compaction, all specimens were moved a into plastic mould whose inner diameter is exactly same as the split proctor mould and stored in a 100% humidity moist room for curing. Complete details of sample construction and quality check are presented in Kang et al. (2014). BCD and thermal conductivity tests were conducted on the samples after 0, 1, 7, 14, and 28 days. The specimens for UCS tests were constructed by the static compression method (Kang et al., 2014). Both treated and untreated soil samples were built at optimum moisture content in accordance with the data from the standard proctor test (ASTM D698) with a specimen size of 71.1 mm diameter and 142.2 mm height. Each specimen was statically compressed in five equal layers in a cylindrical mould. Afterwards, specimens were carefully extruded for immediate BCD modulus tests/thermal conductivity tests or wrapped with a plastic wrap, double sealed in zip-lock plastic bags, and then stored in 100% humidity moist room for curing. For each test, two identical specimens were prepared and the test results were compared so as to statistically minimise the experimental errors and ensure good data quality.

Testing procedures

UCS testing

UCS was determined in accordance with ASTM D 2166 for the chemically stabilised soils. Test specimens were cured at 0, 1, 7, 14, and 28 days, until the treated samples get enough time to set and be strengthened, and to determine the effect of curing length on the UCS. The strain rate was kept at 0.21% per minute until specimen failure.

BCD testing

The BCD is a simple, small-strain, non-destructive testing apparatus that can be used to evaluate the modulus of compacted soils (e.g. Briaud, Li, & Rhee, 2006). A thin plate inside the BCD is in contact with the soil specimen and subjected to a small load that is non-destructive. The measured deflection of the plate is then used to calculate the so-called low-strain BCD modulus (The modulus obtained with the BCD corresponds to a reload modulus, the strain level is at 10^{-3}, stress level at 50 kPa, and time of loading about 2 s).

Thermal conductivity testing

The thermal conductivity, K, is the property of a material to conduct heat. Several methods of determining the thermal properties of soils have been explored including the single probe, dual probe heat pulse, and thermo-time domain reflectometry probe (Abu-Hamdeh, & Reeder, 2000; Ochsner, Horton, & Ren, 2001). In this study, a Decagon Devices KD2 Pro Thermal Properties Analyser was used to record all the thermal conductivities of the soil. The KD2 Pro Analyser consists of a handheld controller and sensors that can be inserted into the soil specimen (Figure 2). A dual-needle SH-1 sensor was used to obtain all the thermal conductivity data in this study. Heat is applied to the heated needle for a set heating time and temperature is measured in the monitoring needle (Figure 2). The readings are then processed by subtracting the ambient temperature at time 0, multiplying by 4π, and dividing by the heat per unit length based on the transient line source method which measures the temperature profile $T(t, r)$at a distance r at time t:

$$T(t,r) = \frac{Q}{4\pi\lambda} E_i\left(\frac{r^2}{4a't}\right), \tag{1}$$

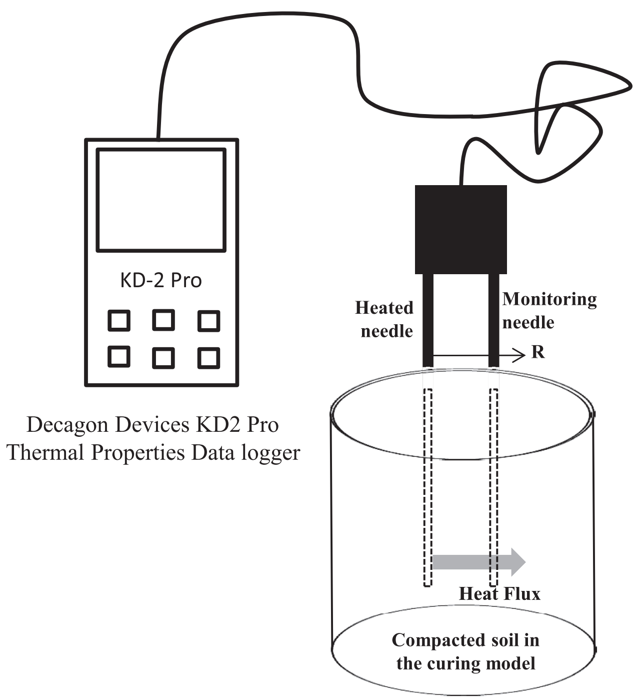

Figure 2. A schematic view of the decagon devices KD2 Pro Thermal Properties Analyser and test set-up.

where Q is the power per unit length (W/m), $\lambda$is the thermal conductivity of the sample (W/mK), a is the thermal diffusivity (m^2/s), and $E_i(x)$is the exponential integral. When performing an experiment which measures the temperature at a point at a fixed distance, the exponential integral can be approximated by the relation: $E_i(x) = -\gamma - \ln(x) + O(x^2)$, where $\gamma \approx 0.5777$ is the Euler gamma constant; thus,

$$T(t, r) = \frac{Q}{4\pi\lambda}\left\{-\gamma - \ln\left(\frac{r^2}{4a}\right) + \ln(t)\right\}. \tag{2}$$

For a given material, the first two terms in the brackets are constant; thus, thermal conductivity can be determined from the slope of $\Delta T - \ln(t)$curve.

Results

Moisture density relationship

Results obtained from the proctor compaction tests of both treated and untreated soils are presented in Figure 3. Each test was performed within 30 min after initial mixing. The addition of FA was found to increase the maximum dry unit weight of the treated soil. The reason for the maximum dry unit weight increase was believed to be due to the squeezing of the finer particles of FA (normally smaller than #200 sieve) into the voids of soil particles (silts and sand) during compaction, thus resulting in an increase in the maximum dry density (McMains & Arman, 1989). The unit weight of LKD was much lower than the soil; therefore, the high percentage ratio of LKD added to soil, the lower the mixture's dry unit weight.

Unconfined compressive strength

The UCS test results of chemically treated soils are shown in Figures 4 and 5. The UCS increased with the FA content increase. The UCS at initial blending of 10 wt% FA sample was 181.2 kPa, as the curing time increased, the UCS increased gradually. When the 28 days of curing time was reached, all the UCS has gained the highest strength. The 10% FA sample gained its most of the strength at about 28 days; however, 15 and 20 wt% FA gained most of the strength at approximately between 14 and 28 days. This indicates that the rate of strength gain is dependent on the

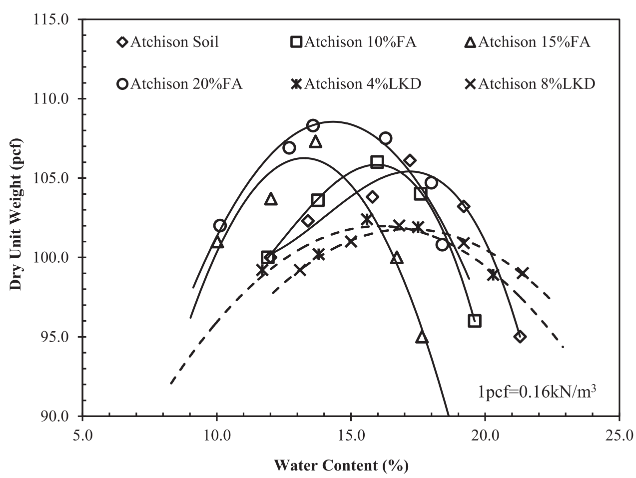

Figure 3. Moisture density relationship of the modified soils.

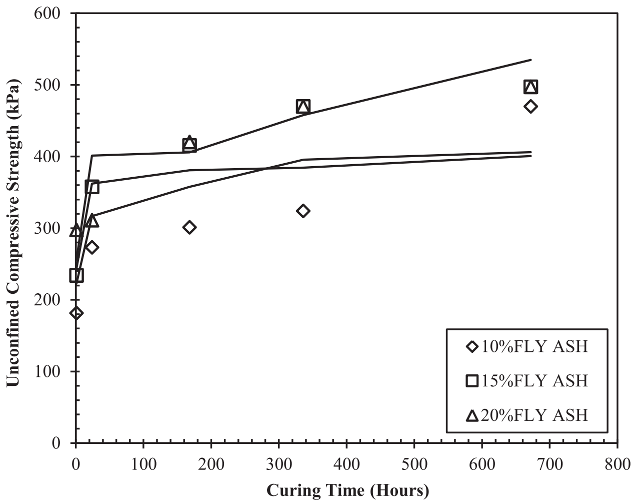

Figure 4. The UCS versus curing time of FA stabilized soils.

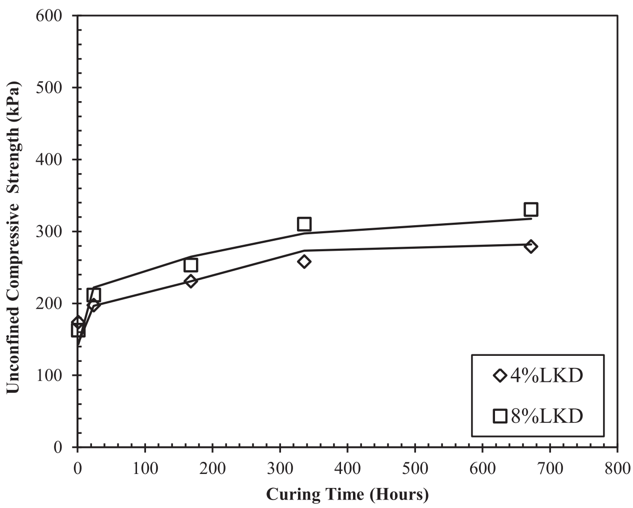

Figure 5. The UCS versus curing time of LKD stabilised soils.

FA content. In other words, the trend indicated that the speed of the sample stiffening increased as the FA content increased. The extra "addition of FA", however, did not influence the final UCS because all the samples have almost the same UCS at 28 days of curing. If given enough time for soils to react with the FA, 10, 15 and 20 wt% FA samples would have approximately the same final UCS. Figure 5 shows the efficiency of the LKD in stabilising the clays. Similarly to the FA-treated soil, as the LKD ratio and curing time increased, the UCS of the LKD treated soil also increased. The LKD treated soil gained most of its strength between 7 and 14 days, after which the strength increase was relatively slow. The black lines in the figures were model-fitted data; the details of the proposed models are shown in the discussion section.

Modulus from the BCD

Figure 6 shows the relationship between BCD modulus and water content under standard proctor compaction effort. The BCD modulus of pure Atchison soil decreased as the water content increased. In general, the BCD modulus of FA–soil mixtures had a "back bone" relationship with the water content (see Figure 6). As the water content increased, the compacted soil gradually changed into the "wet-side", where the inter-particle pores were filled by water and the soil

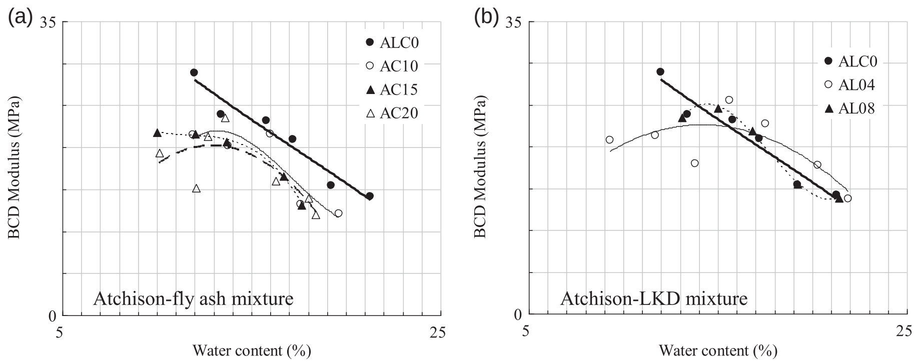

Figure 6. BCD modulus of treated and untreated soils at initial mixing.

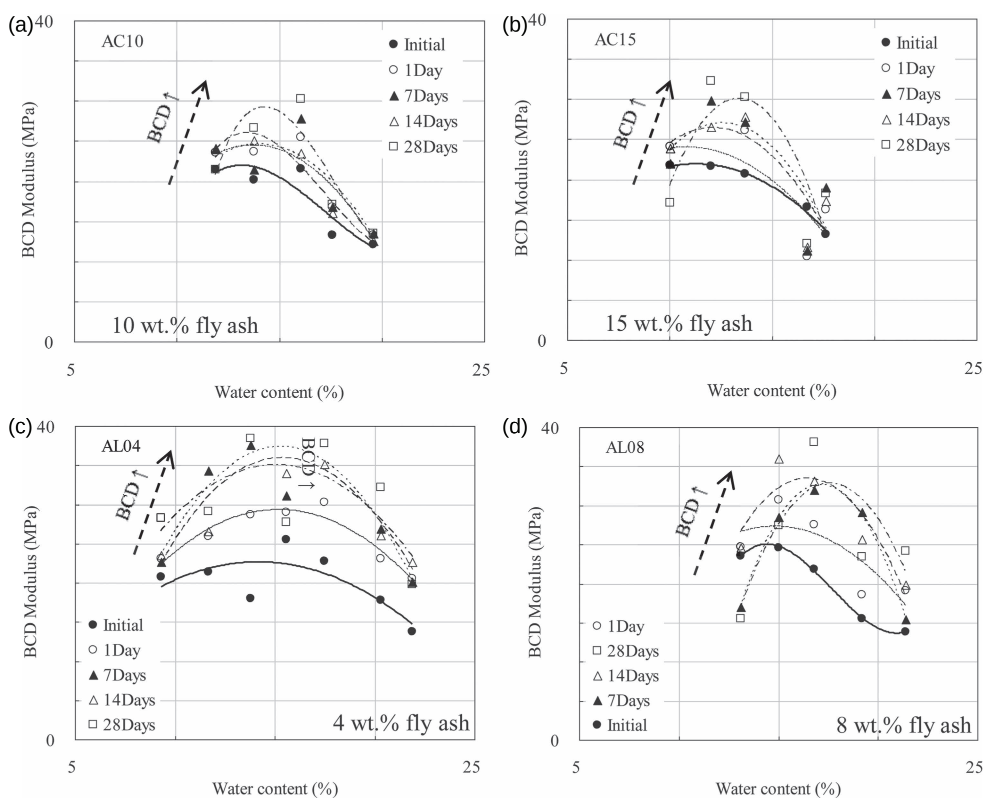

Figure 7. BCD modulus of FA and LKD mixtures at different curing times.

matrix suction decreased. At a macro scale, the soil became "softer" and as a result, the BCD modulus decreased.

Figure 7 shows the BCD modulus of FA and LKD treated soil at different curing periods (0, 1, 7, 14, and 28 days). For 10% FA–soil mixture, the BCD modulus increased as the curing time increased. The maximum BCD modulus was observed at 28 days. A similar trend was found for the 15 and 20 wt% FA–soil mixtures. The modulus of both (4 and 8 wt%) LKD treated

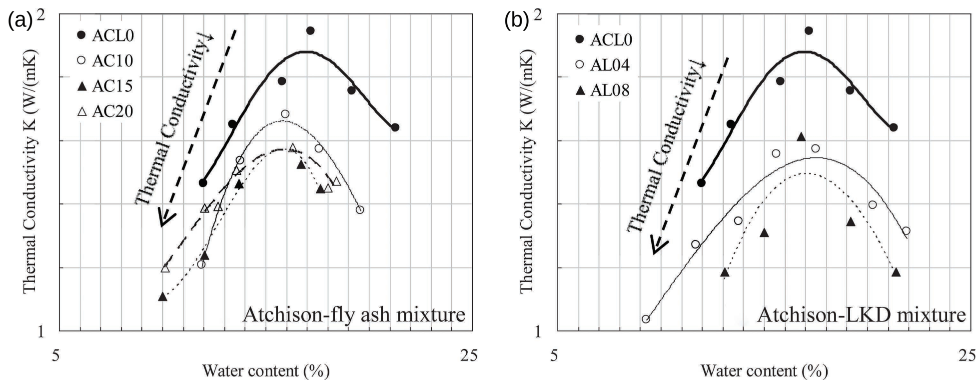

Figure 8. Thermal conductivity of both treated and untreated soils.

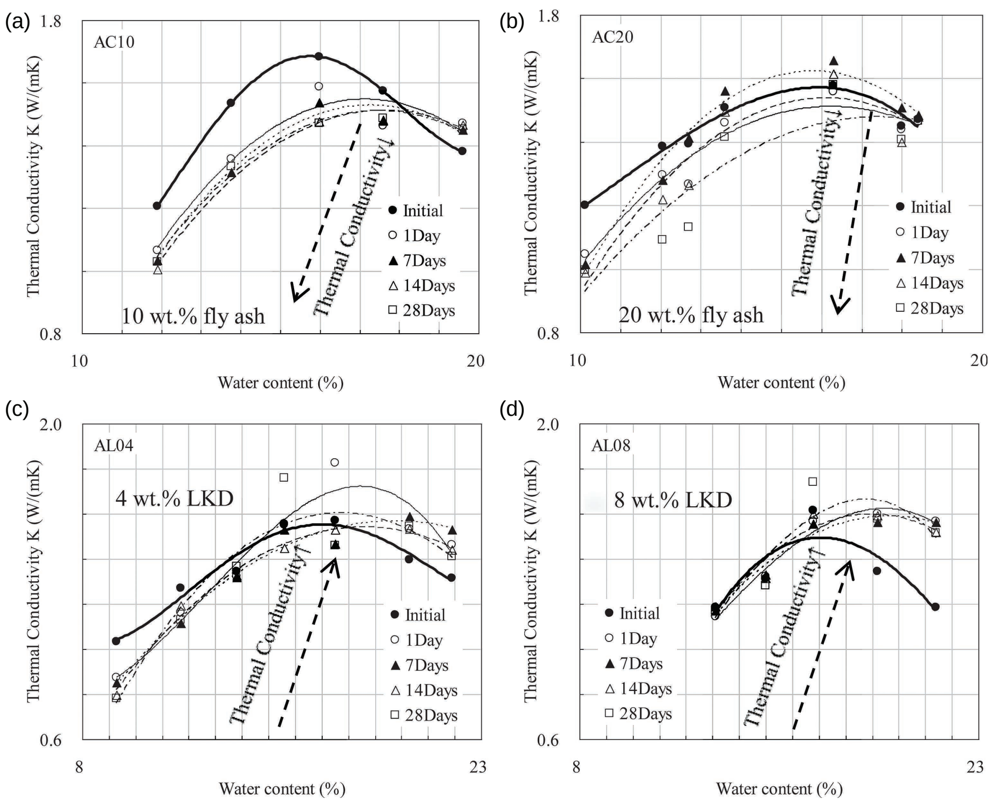

Figure 9. Thermal conductivity of FA and LKD mixtures.

specimens increased with curing time; however, after 14 days of curing, the modulus increase was not apparent.

Thermal conductivity

The relationship between thermal conductivity and water content of FA and LKD treated soil specimens at initial mixing are shown in Figures 8 and 9. The maximum value was observed on pure Atchison soil. With the increase in FA and LKD, the thermal conductivity decreased. When FA was more than 15 wt%, the maximum value became almost constant. The thermal conductivity was significantly decreased by the addition of 4 wt% LKD, but the value was slightly decreased for 8 wt% LKD.

The thermal conductivity of 10 wt% FA–soil mixture was large initially (1.68 W/mK Figure 9(a)) and then decreased as the curing time increased. After about 14 days, all the measured thermal conductivity values became constant. Similar findings were obtained for 15 and 20 wt% FA–soil mixtures. However, the thermal conductivity for the LKD mixture increased with curing time for both 4 and 8 wt% LKD.

Discussions

The upper-and-lower bound of FA–soil mixtures' thermal conductivity

The FA stabilised soil could be treated as a composite material that is consisted by two separate materials, namely the basic soil and the addition FA, of which the physical and mechanical properties are a combination of the two materials' own properties. Therefore, the rules of mixtures which have been used extensively in material science might be employed to understand the composite's upper-and-lower bound thermal conductivities. Both the parallel model and the series model were employed to predict the upper-and-lower bound of the thermal conductivity of the FA–soil mixtures:

$$K_{\mathrm{FA-Soil}} = K_{\mathrm{Soil}} V_{\mathrm{Soil}} + K_{\mathrm{FA}} V_{\mathrm{FA}}, \tag{3}$$

the parallel model – upper bound of the thermal conductivity**

$$\frac{1}{K_{\mathrm{FA-Soil}}} = \frac{V_{\mathrm{Soil}}}{K_{\mathrm{Soil}}} + \frac{V_{\mathrm{FA}}}{K_{\mathrm{FA}}}. \tag{4}$$

the series model – lower bound of the thermal conductivity. Here, K denotes the thermal conductivity and V is the volume fraction of the FA and soil grains in the composite (specific gravity is needed to calculate the volume fraction of each component in the parallel and series models). The thermal conductivity of pure FA over curing time was measured and is displayed in Figure 10. The thermal conductivity was at its peak after initial mixing. As the FA set, its thermal conductivity decreased. By using the parallel and series models, the upper-and-lower bound of the FA stabilised soil mixtures' thermal conductivity values are calculated and plotted in Figure 11. The measured thermal conductivity of the mixtures at different curing periods is also plotted in Figure 11 which is located right between the upper-and-lower bound of the predicted range. Therefore, the results indicated that the two models are applicable for estimating the upper-and-lower bound of the thermal conductivity of FA stabilised soils.

Proposed models for non-destructive testing evaluation

This section is aimed at establishing non-destructive testing based models to predict the UCS of stabilised soil and check the compaction quality in field. In the literature, the ageing of

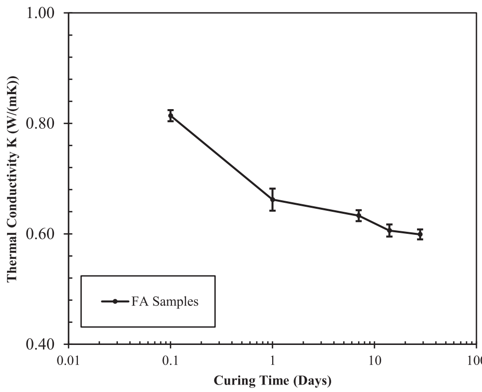

Figure 10. Measured thermal conductivity of pure FA during setting at room temperature.

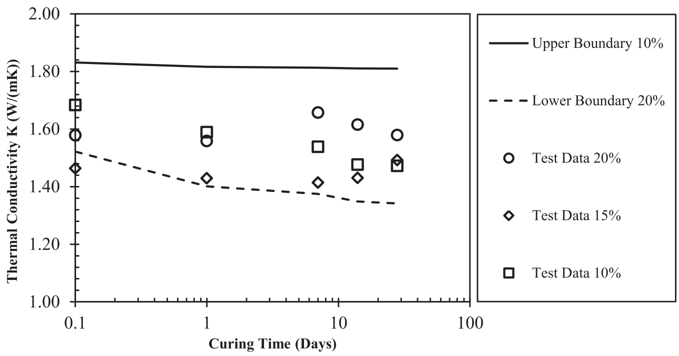

Figure 11. The upper and lower thermal conductivity boundaries of the FA–soil mixtures.

cement-based/modified clay has been investigated by many practitioners (e.g. Chitambira, 2004; Kamruzzaman et al., 2009). Most of these pioneer works were focused on the ageing effects of the strength gain. Curing time was used as an input variable to predict the UCS of stabilised soils (Chitambira, 2004). Except time, other factors such as cement percentage, water content, and density were incorporated to improve the prediction of the UCS. However, most of the published models relied only on the fitting parameters. One disadvantage of these models is that the fitting parameters are largely dependent on the type of soil and stabiliser, which in turn significantly affect the uncertainty of the predicted UCS. Literature review showed that the USC has close relationship with the stiffness and packing state (Chitambira, 2004; Kamruzzaman et al., 2009; Kang et al., 2014; Sunitsakul, Sawatparnich, & Sawangsuriya, 2012). The thermal conductivity was found to be influenced by the porosity and density (Hotz & Ge, 2010). Therefore, it is assumed that the UCS increased exponentially with curing time (Chitambira, 2004) and was influenced by the BCD modulus and thermal conductivity development. By correlating USC with non-destructive testing results, as shown in Equation (5), the prediction of the USC would be achieved. Since the BCD small-strain modulus and thermal conductivity are two basic properties of the stabilised soil, it is reasonable to select the BCD modulus and thermal conductivity to evaluate and predict the UCS gain versus curing time. In this research, a thermal–small-strain stiffness coupled model (Equation (5)) was proposed to predict the UCS of a stabilised soil. The BCD modulus and thermal conductivity were also incorporated in an empirical model which served as a non-destructive testing method to check the compaction quality in field (Equation (6)).

$$q_u = \frac{\mathrm{BCD_{Mixture}}}{\mathrm{BCD_{Soil}}} \frac{K_{\mathrm{Soil}}}{K_{\mathrm{Mixture}}} \exp\left\{a\left[1-\exp\left(\frac{\mathrm{Ash}}{\mathrm{Soil}} - b\ln t\right)\right]\right\}, \tag{5}$$

$$\frac{\rho_{\mathrm{d}}}{\rho_{\mathrm{dmax}}} = c\frac{\mathrm{BCD}}{\mathrm{BCD_{opt}}} + d\frac{K_{\mathrm{opt}}}{K}, \tag{6}$$

where $\mathrm{BCD_{mixture}}$is the BCD modulus of the FA–soil mixture at curing time t. $\mathrm{BCD_{Soil}}$ and $\mathrm{BCD_{opt}}$ are the BCD modulus of the soil and FA–soil mixture at optimum water content and maximum dry unit weight conditions. K_{Soil} and K_{opt} are the thermal conductivity of the soil and FA–soil mixture at the optimum water content and maximum dry unit weight conditions. K_{Mixture} is the thermal conductivity of the FA–soil mixture at curing time t. Ash/Soil is the weight percentage ratio of FA over soil. ρ_{d} is the dry unit weight of a soil or FA–soil mixture. $\rho_{\mathrm{d\,max}}$is the maximum dry unit weight at optimum water condition.

In Equation (5), a and b are the fitting parameters that are based on the type of stabilisers. The fitting parameter a governs the final USC of a chemically treated soil (when curing time equals to infinity); fitting parameter b governs how fast the USC grows over curing time. The normalised BCD modulus and normalised thermal conductivity were found to have correlations with the final USC, and the ash to soil ratio was found to influence the USC growing speed.

In Equation (6), c and d are the fitting parameters based on the non-destructive testing data. The physical meanings of c and d represent the degree of correlation of BCD modulus and thermal conductivity improvement with the dry unit weight of a stabilised soil. For example, the higher the value of c, the closer the relationship between BCD modulus improvement and dry unit weight increase, and vice versa.

The UCS of a chemically treated soil is dependent on the curing time. Other than curing time, the chemical content was found to influence the speed of strength gain. The proposed model incorporated non-destructive testing results to calibrate the prediction of UCS gain over time. The fitting parameters a and b in Equation (5) could be obtained from a curve-fitting technique by using the Solver Add-in in the Microsoft Excel. The combination of a and b that gives the least sum of square error is chosen for the fitting values. For FA treated soil (as shown in Equation (7)), the values of a and b are 5.36 and 36.59, respectively. For LKD treated soil, the values of a and b were 4.82 and 179.39 (in Equation (8)). For both the FA and LKD treated soil, the a values were approximately the same (FA treated sample had a slightly higher value of a, indicating that the final UCS of FA treated soil is slightly higher than that of the LKD treated soil); however, the b values of LKD treated soil were much higher. This big difference indicated that the LKD treated soil had a much faster speed of strength gain compared with the FA treated soil. Model predicted data and test data are presented in Figure 12. Black solid circles represented the UCS of FA treated soil, and hollow circles represented the LKD treated soil. As displayed in the figure, most of the data was located near the diagonal line, indicating that the model predictions were pretty close to the test data (coefficient of determination $R^2 = 0.8239$). Therefore, by carrying out the BCD and thermal conductivity test measurements, the corresponding UCS of a chemically treated soil could be easily predicted.

$$q_u = \frac{\mathrm{BCD_{Mixture}}}{\mathrm{BCD_{Soil}}} \frac{K_{\mathrm{Soil}}}{K_{\mathrm{Mixture}}} \exp\left\{5.36\left[1-\exp\left(\frac{\mathrm{Ash}}{\mathrm{Soil}} - 36.59\ \ln\ t\right)\right]\right\}, \tag{7}$$

$$q_u = \frac{\mathrm{BCD_{Mixture}}}{\mathrm{BCD_{Soil}}} \frac{K_{\mathrm{Soil}}}{K_{\mathrm{Mixture}}} \exp\left\{4.82\left[1-\exp\left(\frac{\mathrm{LKD}}{\mathrm{Soil}} - 179.39\ \ln\ t\right)\right]\right\}. \tag{8}$$

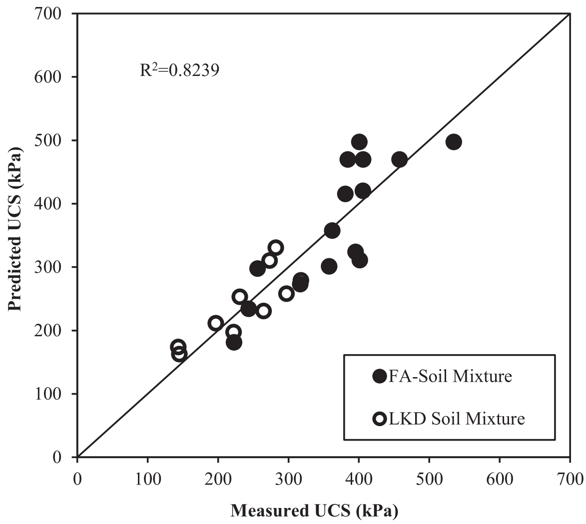

Figure 12. The predicted and measured UCS of the FA and LKD stabilised soil.

The values of *c* and *d* in Equation (6) were obtained from the same curve-fitting technique by using the Solver Add-in in the Microsoft Excel. For the FA treated soil (Equation (9)), the values of *c* and *d* were 0.451 and 0.618, respectively. For the LKD treated soil (Equation (10)), the values of *c* and *d* were 0.521 and 0.568, respectively. For both the FA and LKD treated soil, the values of *c* and *d* were approximately between 0.4 and 0.6, which indicated that the correlation degree of BCD modulus (with the dry density) and thermal conductivity (with the dry density) is almost the same. The model predicted data and test data are presented in Figure 13. Black solid circles represented the FA treated soil and hollow circles represented the LKD treated soil. As presented in the figure, most of the data points were located near the diagonal line, which indicated that the model predictions were pretty close to the test data (coefficient of determination,

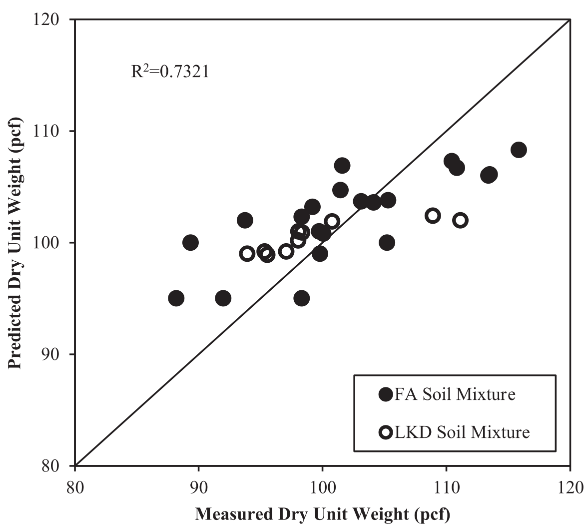

Figure 13. The predicted and measured dry unit weight of the FA and LKD stabilised soils.

$R^2 = 0.7321$). Therefore, the compaction quality check results could be obtained by using the aforementioned equation to carry out the BCD and thermal conductivity test measurements:

$$\frac{\rho_d}{\rho_{d\max}} = 0.451\frac{\mathrm{BCD}}{\mathrm{BCD_{opt}}} + 0.618\frac{K_{\mathrm{opt}}}{K}, \tag{9}$$

$$\frac{\rho_d}{\rho_{d\max}} = 0.521\frac{\mathrm{BCD}}{\mathrm{BCD_{opt}}} + 0.568\frac{K_{\mathrm{opt}}}{K}. \tag{10}$$

Effects of FA and LKD on the UCS and BCD modulus

Test results from mechanical tests, such as moisture density relationship test, unconfined compression test, and BCD modulus test all showed that the FA and LKD could effectively stabilise soft soils, increase the maximum dry unit weight, improve the UCS, and enhance the small-strain modulus.

The mechanism of how FA and LKD stabilise soil has been studied extensively in the literature. The major reason was attributed to the pozzolanic reactions that enhanced the physicochemical bonding between soils and FA particles (Lloyd et al., 2009; Saylak et al., 2008; Shon et al., 2010). Based on the observed test data, the strength and stiffness enhancement of the FA–soil mixture could be categorised into two groups, the short-term strength gain, and long-term strength gain, respectively. The short-term strength gain of FA–soil mixture is usually attributed to the cation exchange process. When FA is added to soil, FA particles react with moisture and start hydration. Due to hydration, large amounts minerals, such as lime (CaO), anhydrite ($CaSO_4$), periclase (MgO), quartz, and tricalcium aluminate are dissolved; thus, the conductivity of the solution increases gradually (see Figure 14). The trivalent cation (Al^{3+}) and divalent cation (Ca^{2+}) available from FA are attracted to clay particles by the cation exchange process. Lower valence cations (H^+, Na^+, and K^+) are replaced by those higher valence cations. The electrolyte concentration in the soil matrix is thus increased and the electrical diffuse double layer (DDL) at the particle–liquid interface is compressed. The adsorption of cation (Al^{3+} and Ca^{2+}) and reduction of the thickness of the DDL promote the particulates to flocculate. Flocculation results in increased pore solution surface tension, producing an increase in apparent cohesion between

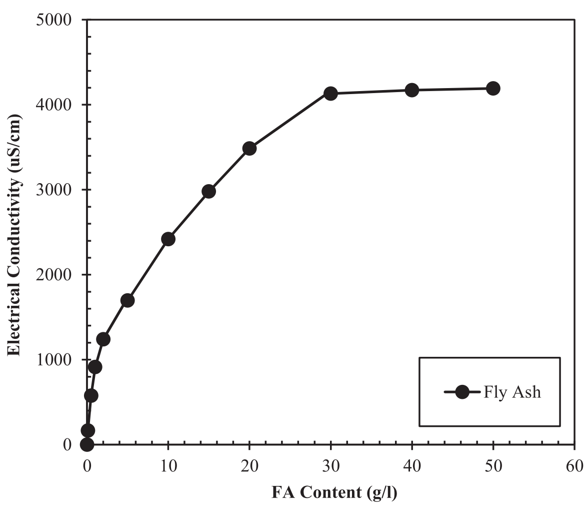

Figure 14. Electrical conductivity change versus FA content.

soil particles, and thus improves the early strength and compatibility. In addition, the reduction of the thickness of the DDL could reduce the repulsion force and increase the van der Waals attraction force among clay particles. The increase in the attractive force is equivalent to an increase in the "effective stress" which will increase the parameters that reflect the resistance of the soil to deformation (Lambe, 1960; Matsui, Ito, Mitchell, & Aben, 1980; Mitchell, 1993; Mitchell & Soga, 2005; Santamarina, Klein, & Fam, 2001; Van Olphen, 1977). This assumption could be directly supported by the increase in the pore fluid conductivity measured from the FA water system (Figure 14), and indirectly supported by the observations of the change in the moisture density relationship and the initial UCS gain. The addition of the FA was found to increase the maximum dry unit weight and the initial UCS.

The long-term strength of the stabilised soil is associated with curing time. The strength gain is attributed to the pozzolanic reactions. Generally the pozzolanic reaction is slow and is even slowed further by the formation of a shell of calcium silicate hydrate (CSH) gel around FA particles (Figure 15). The reaction rate and strength gain are proportional to the consumption of $Ca(OH)_2$. Janz and Johansson (2002) defined pozzolanic material, and the pozzolanic reaction of FA can be briefly described as follows:

$$\mathrm{CaO} + \mathrm{H_2O} \rightarrow \mathrm{Ca(OH)_2}, \tag{11}$$

$$\mathrm{Ca(OH)_2} + \mathrm{Pozzolana} + \mathrm{H_2O} \rightarrow \mathrm{CSH(CASH)}, \tag{12}$$

where CASH is calcium aluminate silicate hydrate.

The BCD modulus increased as the curing time increased, which directly supported that the non-destructive testing method could be used as a fast method to check a compacted soil in the field. As curing time increased, soil particles were gradually bonded with the adjacent particles by the pozzolanic products, which resulted in an increase in the packing density and change in the stress–strain response; thus, the compressibility, strength, and small-strain modulus all increased at the macro scale.

Effects of FA and LKD on the thermal conductivity

Different from the strength properties, thermal conductivity of the treated soil decreased as the curing time increased. This is mainly attributed to the fact that the thermal conductivity of FA is normally lower than that of minerals in natural geomaterials (Figure 10). Meanwhile, as the curing time increases, the thermal conductivity of the FA–soil mixtures decreases gradually. The decrease in the thermal conductivity within the curing time at different FA mixing ratios can be explained by the following mechanisms. Immediately after compaction, the thermal conductivity of the specimens is affected by the addition of FA. As the curing time increases, water is consumed by evaporation and hydration, and a pozzolanic product produced. It is known that the soil thermal properties are strongly influenced by the soil volumetric water content, volume fraction of solids, and volume fraction of air. Air is a poor thermal conductor ($K = 0.026$ W/mK) and reduces the effectiveness of the solid and liquid phases to conduct heat. It is speculated that due to the high degree of pozzolanic reactions, a large portion of the pore water has been consumed, which in turn induces large number of inter-particle pore voids or even some invisible desiccation cracks. The more inter-particle pore voids and invisible cracks developed (equivalent to more air inside), the less the thermal conductivity would be. Scanning electron microscopy (SEM) technique was adopted to verify the microstructure of the FA treated soil. The inter-particle pore voids were clearly seen from the SEM images (see Figure 15), which indirectly supported the decrease in the effective thermal conductivity over curing. Finally, at the end of the curing period, the thermal conductivities of the specimens are governed primarily by the newly formed structures.

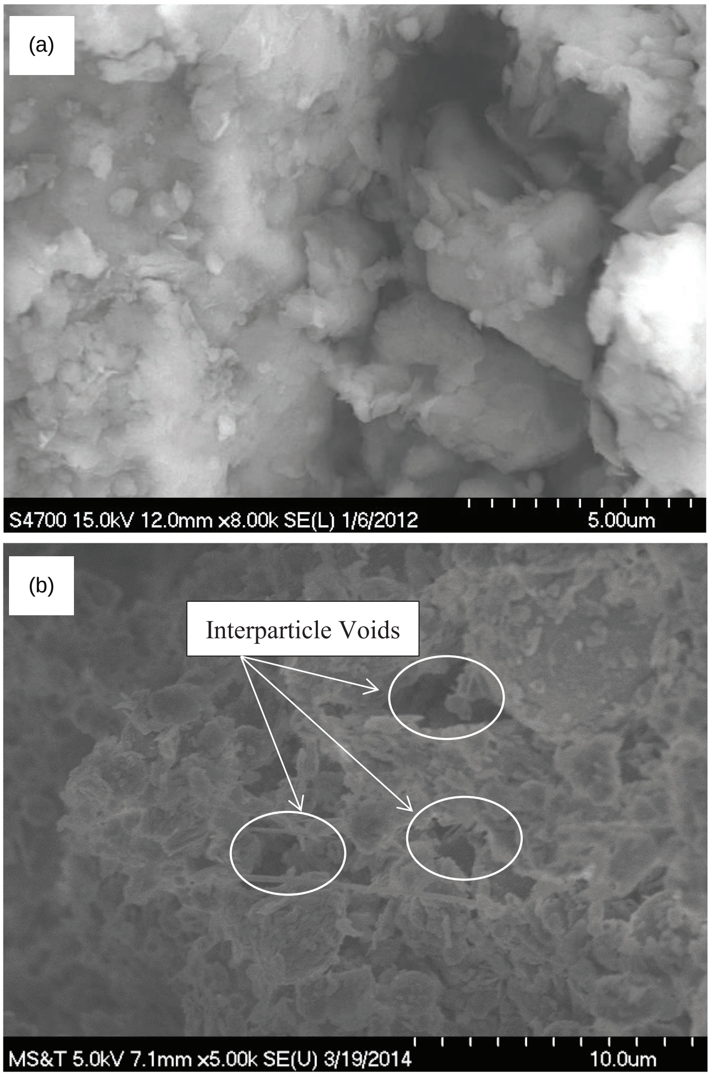

Figure 15. SEM image of FA–soil mixtures at 28 days of curing.

Another possible reason for the decrease in the thermal conductivity might be attributed to the FA and LKD hydration, where metallic ions were released into the pore fluid (indicated by Figure 14). The ions compress the DDL which led to the inter-particle force change. Under this condition, the clay particles flocculated and aggregated with each other, which reduced the specific area of the soil and thus decreased the heat conduction path. Since the FA in general has a lower thermal conductivity (compared with the pure soil), the addition of the FA will also contribute to the reduction of the thermal conductivity of the FA–soil mixtures, because part of the conductive heat path is from soil solids to FA solids. The higher the volume of the FA blending, the lower the resulted effective thermal conductivity will be. This trend was directly supported by the upper and lower boundaries of the thermal conductivity of the FA–soil mixtures (in Figure 11).

Conclusions

Proctor compaction test, unconfined compression test, and non-destructive tests (BCD modulus and thermal conductivity) were carried out on chemically stabilised pavement base soils. Mixing of 20 wt% FA could increase the dry unit weight of the FA–soil mixture from 16.8 to 17.4 kN/m^3 (105.0–108.3 pcf), enhance the UCS from 181.2 to 497.2 kPa (at the end of 28 days of curing), and raise the small-strain BCD modulus up to 40 MPa. Similarly, the 8 wt% of LKD could also effectively improve the UCS up to 330.3 kPa and BCD modulus up to 37 MPa; however, the dry unit weight slightly decreased as the LKD mixing ratio increased. The thermal conductivity decreased as the curing time and stabiliser mixing ratio increased; for instance, the thermal conductivity of 10 wt% FA–soil mixture decreased from 1.67 to 1.47 W/mK at the end of 28 days of curing. Parallel and series models were employed to understand the upper-and-lower bound of the mixtures' thermal conductivity. A thermal strength coupled empirical model which incorporated the non-destructive testing results was developed to predict the UCS strength gain over curing time. In addition, the thermal conductivity and BCD modulus were also incorporated into a novel compaction quality check model. Based on the observed test results, both the models were found to be useful for evaluating the quality of soil stabilisation and offer cost-effective ways for predicting the small-strain modulus in practice.

Disclosure statement

No potential conflict of interest was reported by the authors.

ORCID

Louis Ge http://orcid.org/0000-0002-1150-3733

References

Abuel-Naga, H. M., Bergado, D. T., & Bouazza, A. (2008). Thermal conductivity evolution of saturated clay under consolidation process. *International Journal of Geomechanics*, *8*(2), 114–122.

Abu-Hamdeh, N. H., & Reeder, R. C. (2000). Soil thermal conductivity: Effects of density, moisture, salt concentration, & organic matter. *Soil Science Society of America Journal*, *64*, 1285–1290.

Bachmann, J., Horton, R., Ren, T., & van der Ploeg, R. R. (2001). Comparison of the thermal properties of four wettable and four water-repellent soils. *Soil Science Society of America Journal*, *65*, 1675–1679.

Balland, V., & Arp, P. A. (2005). Modeling soil thermal conductivities over a wide range of conditions. *Journal of Environmental Engineering and Science*, *4*, 549–558.

Brandon, T. L., & Mitchell, J. K. (1989). Factors influencing thermal resistivity of sands. *Journal of Geotechnical Engineering*, *115*(12), 1683–1698.

Brandon, T. L., Mitchell, J. K., & Cameron, J. T. (1989). Thermal instability in buried cable backfills. *Journal of Geotechnical Engineering*, *115*(1), 38–55.

Briaud, J., Li, Y., & Rhee, K. (2006). BCD: A soil modulus device for compaction control. *Journal of Geotechnical and Geoenvironmental Engineering*, *132*(1), 108–115.

Burnham, J. C., Hatfield, N., Bennett, G. F., & Logan, T. J. (1992). Use of kiln dust with quicklime for effective municipal sludge pasteurization and stabilization with the N-Viro Soil process. *ASTM Special Technical Publication*, *1135*, 128–141.

Cetin, B., Aydilek, A. H., & Guney, Y. (2010). Stabilization of recycled base materials with high carbon fly ash Resources. *Conservation and Recycling*, *54*(11), 878–892.

Chitambira, B. (2004). *Accelerated ageing of cement stabilized/solidified contaminated soils with elevated temperatures* (Ph.D. dissertation). University of Cambridge, Cambridge, UK.

Cokca, E. (2001). Use of class C fly ashes for the stabilization of an expansive soil. *Journal of Geotechnical and Geoenvironmental Engineering*, *127*(7), 568–573.

Daita, R. K., Drnevich, V. P., Kim, D., & Chen, R. (2006). Assessing the quality of soils modified with lime kiln dust measuring electrical conductivity with time domain reflectometry. *Transportation Research Record. Journal of the Transportation Research Board*, *1952*, 101–109.
Heckel, G., & Wahab, R. (1996). *Soil stabilization utilizing alternative waste materials*. Proceedings of the Materials Engineering Conference, Washington, DC, 318–327.
Horpibulsuk, S., Rachan, R., & Raksachon, Y. (2009). Role of fly ash on strength and microstructure development in blended cement stabilized silty clay. *Soils and Foundations*, *49*(1), 85–98.
Hotz, R. D., & Ge, L. (2010). Investigation of the thermal conductivity of compacted silts and its correlation to the elastic modulus. *Journal of Materials in Civil Engineering*, *22*(4), 408–412.
Janz, M., & Johansson, S. (2002). *The functions of different binding agents in deep stabilization* (Swedish Deep Stabilization Research Center Rep. No. 9). Linkoping: Swedish Geotechnical Institute.
Kamruzzaman, A. H., Chew, S. H., & Lee, F. H. (2009). Structuration and destructuration behavior of cement-treated Singapore marine clay. *Journal of Geotechnical and Geoenvironmental Engineering*, *135*(4), 573–589.
Kang, X., Kang, G., & Ge, L. (2013). Modified time of setting test for fly ash paste and fly ash-soil mixtures. *Journal of Materials in Civil Engineering*, *25*(2), 296–301.
Kang, X., Kang, G-C., Chang, T-K., & Louis, G. (2014). Chemically stabilized soft clays for road base construction. *Journal of Materials in Civil Engineering*. doi:10.1061/(ASCE)MT.1943-5533.0001156
Lambe, T. W. (1960). *A mechanistic pic of shear strength of clay*. Proc. research conf. on shear strength of cohesive soils, ASCE, New York, 555–580.
Lloyd, R. R., Provis, J. L., & van Deventer, J. S. J. (2009). Microscopy and microanalysis of inorganic polymer cements.2: The gel binder. *Journal of Materials Science*, *44*, 620–631.
Matsui, T., Ito, T., Mitchell, J. K., & Aben, N. (1980). Microscopic study of shear mechanisms in soils. *Journal of the Geotechnical Engineering Division, ASCE*, *106*(2), 137–152.
McManis, K. L., & Arman, A. (1989). Class C fly ash as full or partial replacement for Portland cement or lime. *Transportation Research Record*, *1219*, 68–81.
Miller, M. M., & Callaghan, R. M. (2004). *Lime kiln dust as a potential raw material in Portland cement manufacturing* (Department of the Interior Geological Survey Open-File Report 2004–1336). Retrieved from http://pubs.usgs.gov/of/2004/1336/2004-1336.pdf
Misra, A. (1998). Stabilization characteristics of clays using class C fly ash. *Transportation Research Record*, *1611*, 46–54.
Mitchell, J. K. (1993). *Fundamentals of soil behaviors* (2nd ed.). New York, NY: John Wiley and Sons.
Mitchell, J. K., & Soga, K. (2005). *Fundamentals of soil behavior* (3rd ed.). New York, NY: John Wiley and Sons, 577pp.
Ochsner, T. E., Horton, R., & Ren, T. (2001). A new perspective on soil thermal properties. *Soil Science Society of America Journal*, *65*, 1641–1647.
Puppala, A. J., Ramakrishna, A. M., & Hoyos, L. R. (2003). Resilient moduli of treated clays from repeated load triaxial test. *Transportation Research Record*, *1821*, 68–74.
Santamarina, J. C., Klein, K. A., & Fam, M. A. (2001). *Soils and waves – particulate materials behavior, characterization and process monitoring*. New York, NY: John Wiley and Sons.
Saylak, D., Mishra, S. K., Mejeoumov, G. G., & Shon, C-H. (2008). Fly ash-calcium chloride stabilization in road base construction. *Transportation Research Record: Journal of the Transportation Research Board*, *2053*, 23–29.
Shon, C-H., Saylak, D., & Mishra, S. K. (2010). Combined use of calcium chloride and fly ash in road base stabilization. *Transportation Research Record: Journal of the Transportation Research Board*, *2186*, 120–129.
Solanki, P., Zaman, M. M., & Dean, J. (2010). Resilient modulus of clay subgrades stabilized with lime, class C fly ash, & cement kiln dust for pavement design. *Transportation Research Record: Journal of the Transportation Research Board*, *2186*, 101–110.
Sunitsakul, J., Sawatparnich, A., & Sawangsuriya, A. (2012). Prediction of unconfined compressive strength of soil-cement at 7 days. *Geotechnical and Geological Engineering*, *30*(1), 263–268.
Tan, T. S., Goh, T.-L., & Yong, K.-Y. (2002). Properties of Singapore marine clays improved by cement mixing. *Geotechnical Testing Journal*, *25*(4), 422–433.
Tuncer, B. E., Hector, A., & Craig, H. B. (2006). Stabilizing soft fine-grained soils with fly ash. *Journal of Materials in Civil Engineering*, *18*, 283–294.
Van Olphen, H. (1977). *Clay colloid chemistry* (2nd ed.). New York, NY: Wiley.
Weidinger, D. M., & Ge, L. (2009). Laboratory evaluation of the Briaud compaction device. *Journal of Geotechnical and Geoenvironmental Engineering*, *135*(10), 1543–1546.